IEEE Access
Multidisciplinary | Rapid Review | Open Access Journal

Received November 2, 2017, accepted December 7, 2017, date of publication December 12, 2017, date of current version March 9, 2018.

Digital Object Identifier 10.1109/ACCESS.2017.2782686

Handmade Trileaflet Valve Design and Validation for Pulmonary Valved Conduit Reconstruction Using Taguchi Method and Cascade Correlation Machine Learning Model

CHUNG-DANN KAN[1], WEI-LING CHEN[2], CHIA-HUNG LIN[3,4], JIEH-NENG WANG[5], PONG-JEU LU[6], MING-YAO CHAN[7], AND JUI-TE WU[7]

[1]Division of Cardiovascular Surgery, Department of Surgery National Cheng Kung University Hospital, College of Medicine, National Cheng Kung University, Tainan 70101, Taiwan
[2]Department of Engineering and Maintenance, Kaohsiung Veterans General Hospital, Kaohsiung 81362, Taiwan
[3]Department of Electrical Engineering, Kao-Yuan University, Kaohsiung City, 82151, Taiwan
[4]National Chin-Yi University of Technology, Taichung 41170, Taiwan
[5]Department of Pediatrics, National Cheng Kung University Hospital, Tainan 70101, Taiwan
[6]Heart Science and Medical Devices Research Center, National Cheng Kung University, Tainan 70101, Taiwan
[7]Department of Veterinary Medicine, National Chiayi University, Chiayi 60004, Taiwan

Corresponding authors: Chung-Dann Kan (kcd56@mail.ncku.edu.tw) and Chia-Hung Lin (eechl53@gmail.com)

ABSTRACT Pulmonary valve diseases in children and adults include different degrees of stenosis, regurgitation, or congenital defects. Valve repair or replacement surgery is used to treat valvular dysfunction and to improve regurgitations flow for pulmonary valve pathologies. Handmade trileaflet valve designs with different ranges of diameters have been used for pulmonary valved conduit reconstruction among children or adult patients with available conditions. In this paper, we propose a multiple regression model as a cascade-correlation-network-based estimator to determine optimal trileaflet parameters, including width, length, and upper/lower curved structures, for trileaflet valve reconstruction. The diameter of the main pulmonary artery is determined via computed tomography pulmonary angiography, and a trileaflet valve template is rapidly sketched. The actual valve is constructed using an expanded polytetrafluoroethylene material. Using an experimental pulmonary circulation loop system, design parameters and valve efficacy can be validated by the Taguchi method through calculation of signal-to-noise ratios. Experimental results indicate that in contrast to commercial valve stents, the handmade trileaflet valve exhibits good performance and is a valuable option in treatment of severe pulmonary regurgitation.

INDEX TERMS Handmade trileaflet valve design, valve replacement, cascade correlation network (CCN), Taguchi method, signal-to-noise (S/N) ratio.

I. INTRODUCTION

Right ventricular outflow tract (RVOT) reconstruction is one of the important and distinct procedures for complex congenital heart surgeries. However, right heart failure is not uncommon in patients after treatment for complicated congenital heart diseases involving the RVOT, which can present chronic pulmonary insufficiency, right ventricular dilatation, and ventricular arrhythmias. Pulmonary valve diseases may occur as a result of congenital heart disease, postoperative valve degeneration, or calcium deposition on previous substitutes with aging in children or adults. These diseases may be caused by various pathological abnormalities for the right ventricle, pulmonary artery, or pulmonary parenchyma due to problems, such as valvular stenosis and insufficiency [1], [2], the results of which comprise pressure/volume overload for the right ventricle. Both pulmonary stenosis and regurgitation may occur simultaneously at different degrees and may result in dilation of the right ventricle and subsequent right and left ventricular dysfunction. In addition, congenital heart disease in the early-infant stage may cause valvular degeneration of the pulmonary valve, resulting in blood flow regurgitation, stenosis progression, increases in pulmonary vascular resistance, and right ventricular dysfunction [3]. Patients with these conditions are symptomatic and present high right

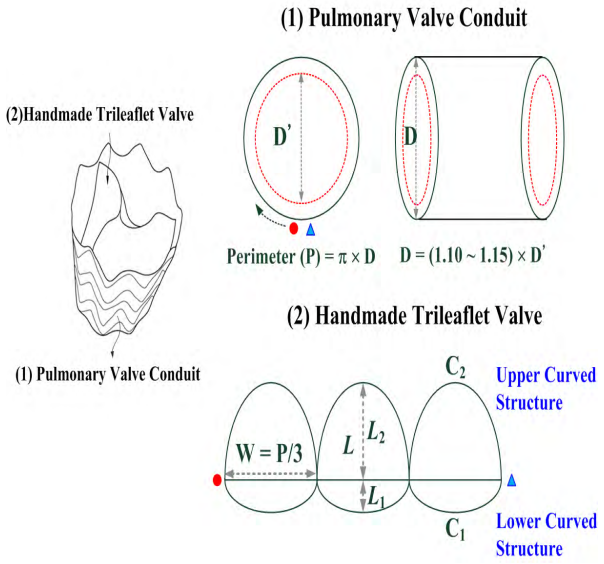

FIGURE 1. The handmade pulmonary trileaflet valve conduit.

ventricular pressure (RVP) (> 60 mmHg) and ventricular cardiac arrhythmia [4], [5]. In clinical settings, qualitative measurements, electrocardiography (ECG) and/or exercise ECG signals, echocardiography, and cardiovascular magnetic resonance images [6]–[8] are applied for early assessment of patient status and evaluating the possible requirement for valve surgery.

Traditionally, patients receive open-heart surgery to repair or to replace the pulmonary valve. Although surgical pulmonary valve surgery is associated with low morbidity and mortality rates, in many instances, operation risks are high, or surgery is prohibitive. Surgery requires a 2- to 5-inch-long surgical wound on the chest wall. By contrast, catheter-based endovascular surgery employs only a puncture wound on the inguinal or neck region, reduces surgical risk, and improves patient care by achieving fast recovery times and short hospital stays. Melody® transcatheter pulmonary valve replacement (TPVR) technique is an approach used to treat narrowed pulmonary valve or leaking valve conduits between the right ventricle and pulmonary artery without the need for open-heart surgery.

Homografts are the most-often used conduits for pulmonary valve replacement. However, these grafts do not ensure the best possible durability as calcification occurs with aging in very young patients. In addition, not all homograft sizes are always available [9]. As shown in Figure 1, previous studies have shown that a handmade expanded polytetrafluoroethylene (ePTFE) trileaflet conduit [9]–[12] provides a suitable alternative procedure for both adult and child patients. ePTFE presents low friction and possesses low tissue affinity [12]–[14]. Therefore, this material can resist valve degeneration and calcification and is thus useful for pulmonary valve replacement. However, in relation to this material, two primary issues, including size restrictions and validation of valved conduit efficacy, must be resolved. Determining size and diameter of the trileaflet before TPVR is necessary, and functions of replacement valved conduit should be analyzed to verify hemodynamic status, valve efficacy, and cardiac output (CO). Hence, this work proposes an assistant tool for the design of handmade trileaflet valves for pulmonary valve reconstruction. The functions of the handmade valve are then validated under different heart rates (HRs), blood flow volumes, and hypertension conditions using the Taguchi method.

In the handmade pulmonary valved conduit shown in Figure 1, the diameter (D) of the conduit can be obtained through computed tomography (CT) pulmonary angiography measurement. D is generally oversized in comparison with the original diameter, D' (10%–15% larger); as a result, the conduit lands in the main pulmonary artery as closely as possible [15], [16]. A thin ePTFE membrane is then trimmed into a semilunar tricuspid shape. Width (W) of each leaflet is one-third of the perimeter (P). Both D and W are known leaflet parameters, and length ($L = L_1 + L_2$) and bisemilunar tricuspid shape (C_1 and C_2, respectively) of each leaflet are approximately proportional to D. Lower and upper curved structures of the leaflets can be modified by varying D and W.

We propose a machine learning model as a cascade-correlation-network (CCN) [17]–[19]-based estimator to determine the optimal trileaflet parameters. For finite experimental runs, typical input–output paired training data, $(D, W) - (L_1, L,$ and $\mu)$, are selected using the Taguchi method and then established to train the *CCN*-based estimator. This model is designed as a multiple regression estimator with an interpolation function to determine optimal trileaflet parameters, including L_1, L, and μ. Next, using an example pulmonary circulation loop system, the Taguchi method is used to evaluate pulmonary valve efficiency via several signal-to-noise (S/N) ratios, including nominal-the-best (S/N_{NTB}), larger-the-better (S/N_{LTB}), and smaller-the-better (S/N_{STB}) ratios [20]–[23]. Experimental results show that in comparison with commercial valve stents, the proposed handmade trileaflet valve replacement features significant improvement, as evidenced by observable decreases in regurgitation and increases in valve efficacy.

II. METHODOLOGY

A. HANDMADE TRILEAFLET VALVE DESIGN

Figure 2 shows a template of a handmade leaflet, which can be sketched using geometric shapes consisting of lower and upper curved lines, C_1 and C_2, and two straight lines, C_3 and C_4. These geometric lines can be presented as follows [24]:

Two curved lines:

$$C_1(x) = \frac{x^2}{8 \times (D/20) \times L_1}, \quad x \in [-\mathrm{W}_1, +\mathrm{W}_1] \tag{1}$$

$$C_2(x) = \frac{x^2}{-\mu \times (D/20) \times L_1} + L, \quad x \in [-W_1, +W_1] \tag{2}$$

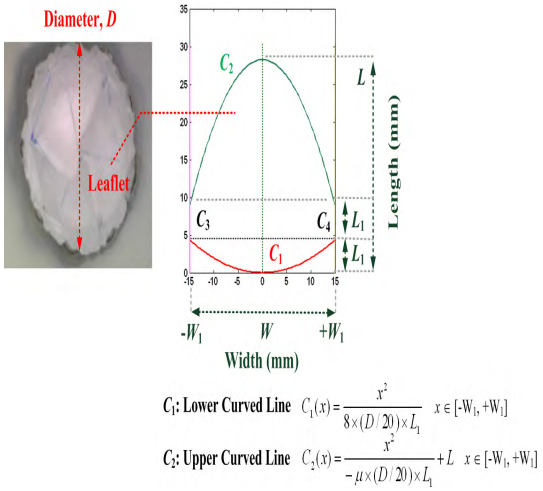

FIGURE 2. The geometric shape of each leaflet and the key parameters for semilunar tricusp design.

Two vertical lines:

$$x = -W_1, \quad C_3(x) \in [L_1, 2L_1] \tag{3}$$

$$x = +W_1, \quad C_4(x) \in [L_1, 2L_1] \tag{4}$$

where D (mm) refers to the diameter of the pulmonary valved conduit; length L_1 is the connecting junction (usually 3.0–5.0 mm) at the lower curved structure [10]; W corresponds to the width (mm) of each leaflet, $W = +W_1 - (-W_1) = 2 \times W_1$; and L is the length (mm) of each leaflet. The width of each leaflet is one-third of $P = (\pi \times D)/3$. Based on the 20 mm diameter commonly observed in children, two terms, $[8 \times (D/20)]$ and $[-\mu \times (D/20)]$, can be employed to modify the lower and upper curved lines and obtain different valve diameters (e.g., $\mu \approx 2.1$–1.9 for children and $\mu \approx 1.9$–1.50 for adults) [24].

D and W are known parameters, and L can be estimated using the following:

$$L = \left|\frac{x^2}{-\mu \times (D/20) \times L_1}\right| + 2 \times L_1, \quad x \in [-\mathrm{W}_1, +\mathrm{W}_1] \tag{5}$$

where the curved parameter, μ, is used to control the length of the upper curved line. In Table 1, we establish specific leaflet templates for children and adults. The proposed template (standard template) has been evaluated by clinicians [10], [24] and observed to correlate with parameters D and W and optimal parameters L_1, L, and μ for our handmade trileaflet valve design.

In this study, the Taguchi method [20]–[23] is applied to provide predictive knowledge on multi-variable processes with a limited number of trials using parameters L_1, L, and μ. The method uses the loss function to measure performance characteristics that deviate from desired target values. Then, the value of this loss function is transformed into S/N ratios, including S/N_{NTB}, S/N_{LTB}, and S/N_{STB} [20]–[23]. These S/N ratios are used to evaluate pulmonary valve efficiency via the regurgitation fraction (RF) and heart

TABLE 1. Specific standards for establishing input–output paired training data.

D (mm)	W (mm)	L_1 (mm)	L (mm)	μ
18.00	18.84	3.60	20.24	2.10
20.00	20.93	3.80	22.01	2.00
22.00	23.03	4.00	23.85	1.90
24.00	25.12	4.20	25.79	1.80
26.00	27.21	4.40	27.83	1.70
28.00	29.31	4.60	30.03	1.60
30.00	31.40	4.80	31.68	1.55
32.00	33.49	4.80	33.94	1.50
34.00	35.58	4.80	35.47	1.50
36.00	37.68	5.00	36.29	1.50

pump efficiency (HPE). RF index is calculated as the ratio between forward stroke flow and regurgitation flow through the pulmonary valve during each heartbeat. For each heartbeat, end-systolic and end-diastolic volumes are computed by integral operations as follows:

$$SV = \int_{t_1}^{t_2} PAF_{fw} dt \tag{6}$$

$$RV = \int_{t_2}^{t_3} PAF_{rv} dt \tag{7}$$

where SV stands for the forward stroke volume (SV, mL), PAF_{fw} is forward pulmonary arterial flow (PAF) rate during the systolic period $[t_1, t_2]$, RV represents the regurgitation volume (RV, mL), and PAF_{rv} is the regurgitation flow rate during the diastolic period $[t_2, t_3]$. RF index can be presented as follows [25], [26]:

$$RF\% = \frac{|RV|}{|SV| + |RV|} \times 100\%, \quad PAF = |SV| + |RV| \tag{8}$$

where PAF corresponds to total blood volume for one heartbeat ($PAF = 40$, 50, 60 mL in this study). In normal conditions, no blood is regurgitated, indicating that $RF\% \approx 0\%$. During regurgitation, $RF\% \leq 20\%$ indicates moderate regurgitation, and $20\% < RF\%$ and $RF\% < 40\%$ indicate mild and severe regurgitation, respectively. Ideally, RF should be as small as possible. For various combinations of PAFs and HRs, appropriate design parameters (D, W, L_1, L, μ) minimize the objective function as follows:

$$S/N_{STB} = -10 \times \log\left(\frac{1}{N}\sum_{g=1}^{N}(RF\%_g^2)\right) \tag{9}$$

where N is the total number of experimental runs, and $RF\%_g$ is the RF index in the gth running experiment. S/N_{STB} approaching zero is considered optimal. To reduce variability around a mean, $S/N_{RF,NTB}$ is used to evaluate variations in $RF\%$ index as follows:

$$S/N_{RF,NTB} = 10 \times \log\left(\sum_{g=1}^{N}\left(\frac{RF\%_{mean}}{S_{RF}}\right)^2\right) \tag{10}$$

where $RF\%_{mean}$ is the mean response for N experimental runs, and S_{RF} represents the standard deviation. CO is related to the quantity of blood delivered to the right and left lungs

and is also an indicator of *HPE*; the two variables are computed as follows:

$$CO(L/\min) = SV(L/beat) \times HR(beats/\min) \quad (11)$$

$$HPE\% = \frac{Outflow\ Volume}{Inflow\ Volume} \times 100\% = \frac{CO}{PAF \times HR} \times 100\% \quad (12)$$

where *HR* is the HR. $HPE\% \geq 80\%$ indicates good outcomes for HPE; hence, its value should be as large as possible. The optimal design maximizes the objective function as follows:

$$S/N_{HPE,LTB} = -10 \times \log(\frac{1}{N}\sum_{g=1}^{N}(\frac{1}{HPE\%_g^2}) \quad (13)$$

where $HPE\%_g$ is the *HPE* index in the gth running experiment. $S/N_{HPE,NTB}$ is used to evaluate variations in *HPE%* as follows:

$$S/N_{HPE,NTB} = 10 \times \log(\sum_{g=1}^{N}(\frac{HPE\%_{mean}}{S_{HPE}})^2) \quad (14)$$

where $HPE\%_{mean}$ corresponds to the mean response for N experimental runs, and S_{HPE} is the standard deviation.

The specific leaflet templates in Table 1 reflect optimal design parameters for children ($\leq$ 20.00 mm) and adults as determined using Taguchi's method. In contrast to that of commercial valve stents, performance of handmade trileaflet valved conduits can be verified using S/N ratios, S/N_{NTB}, S/N_{LTB}, and S/N_{STB} indices, through experimental biophysical tests. As the input–output paired experimental data in Table 1, i.e., $(D, W) - (L_1, L, \mu)$, have been evaluated by the Taguchi method and clinicians, we can then consider these training data to train the machine learning-based estimator.

B. MACHINE LEARNING BASED ESTIMATOR

For multiple regression applications, the machine learning method is used to map the relationship between two input variables (D and W) and three output variables (L_1, L, and μ). *CCN* [17]–[19] model is applied as an estimator, as presented in Figure 3. *CCN* architecture consists of an input layer, a hidden layer, and an output layer. Input nodes (x_i, $I = 1, 2$) are connected to hidden nodes (Y_j, $j = 1, 2, 3$) via adjustable weight connections, w_{ij}, and these connections from input nodes to any hidden node are trained when a hidden node is added to the network. Given the input–output paired training data, the cascade correlation process starts with a minimal network consisting only of the input layer, hidden layer, and a bias input. When any candidate node is added to the network, all w_{ij} values are automatically adjusted by back-propagation method.

When training stage is completed, all network weights are frozen, and the candidate node becomes a hidden node as the single perceptron. The next hidden node is connected to the network using the same training process. Newly created nodes are independent of the previous ones. Each hidden node can receive information from all input nodes and a bias.

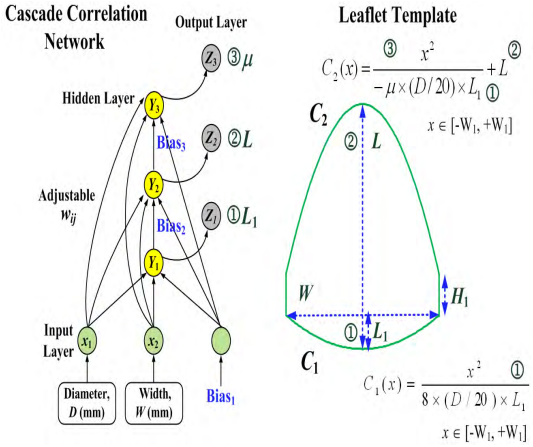

FIGURE 3. The architecture of the *CCN* model.

This machine learning algorithm allows for online learning applications, and processing continues until all hidden nodes are added. The *CCN* model is constructed by adding hidden nodes one by one. Network building requires only a minimum number of hidden nodes and w_{ij}. The algorithm includes a speed learning stage and can construct a multiple regression model. The algorithm of the *CCN*-based estimator is summarized as follows:

Step 1. Establish the input–output paired training data (X_k, Y_k) as the training set of K samples:

$$\text{Input Vector: } X_k = [x_1, x_2] = [\frac{D(k)}{D_{\max}}, \frac{W(k)}{W_{\max}}]^T, \quad k = 1, 2, 3, \ldots, K \ (K = 10 \text{ in this study}) \quad (15)$$

$$\text{Output Vector: } Y_k = [Y_1, Y_2, Y_3] = [\frac{L_1(k)}{L_{1\max}}, \frac{L(k)}{L_{\max}}, \frac{\mu(k)}{\mu_{\max}}, 1]^T \quad (16)$$

where $D_{max} = 36.00$ (mm) and $W_{max} = 37.68$ (mm) are maximum values, as shown in Table 1. In this paper, D ranges from 20.00 mm to 36.00 mm for adult patients and < 20.00 mm for child patients, $L_{1\max} = 5.00$ (mm) and $L_{max} = 36.29$ (mm) are maximum lengths, and $\mu_{max} = 2.10$ is the maximum parameter for sketching the upper curved line. The training set of leaflet parameters is normalized by maximum values. According to Table 1, input–output paired training data can be presented as follows:

$$X \Rightarrow Y: \begin{bmatrix} 0.50 & 0.50 \\ 0.55 & 0.55 \\ 0.61 & 0.61 \\ 0.67 & 0.67 \\ 0.72 & 0.72 \\ 0.78 & 0.78 \\ 0.83 & 0.83 \\ 0.89 & 0.89 \\ 0.94 & 0.94 \\ 1.00 & 1.00 \end{bmatrix} \Rightarrow \begin{bmatrix} 0.72 & 0.56 & 1.00 \\ 0.76 & 0.61 & 0.95 \\ 0.80 & 0.66 & 0.90 \\ 0.84 & 0.71 & 0.86 \\ 0.88 & 0.77 & 0.81 \\ 0.92 & 0.83 & 0.76 \\ 0.96 & 0.87 & 0.74 \\ 0.96 & 0.94 & 0.71 \\ 0.96 & 0.98 & 0.71 \\ 1.00 & 1.00 & 0.71 \end{bmatrix} \quad (17)$$

Step 2. Add the candidate node Y_j by connecting the node Y_j to two input nodes x_1 and x_2 with w_{ij}, $i = 1, 2, j = 1, 2, 3$, and $w_{ij} = 1$ and then set the target output $T_{jk} = Y_k$ with K input–output paired training data $(X_k, Y_k), k = 1, 2, 3, \ldots, K$. Next, compute the output of node Y_j using the radial basis function (activation function) with the following:

$$Bias_j = \begin{cases} 0, & j = 1 \\ \sum_{j=1}^{j-1} 0.1 \times Y_j, & j > 1 \end{cases} \tag{18}$$

$$Y_j = \exp(-\frac{1}{2} \times (\frac{net_j}{\sigma_j})^2), \quad net_j = \sum_{i=1}^{2} (x_i - m_j)^2 + Bias_j \tag{19}$$

where σ stands for the standard deviation, and m_j is the mean value.

Step 3. Given a squared error function, $E(\sigma_j, m_j)$, use the gradient descent algorithm to find the optimal parameters σ_j and m_j to minimize $E(\sigma_j, m_j)$ as follows:

$$E(\sigma_j, m_j) = \sum_{k=1}^{K} (T_{jk} - Y_j)^2 \tag{20}$$

$$\Delta\sigma_j = -1 \times \frac{\partial E(\sigma_j, m_j)}{\partial \sigma_j} = (T_{jk} - Y_j) \times Y_j \times \frac{(net_j)^2}{\sigma_j^3} \tag{21}$$

$$\Delta m_j = -1 \times \frac{\partial E(\sigma_j, m_j)}{\partial m_j} = (T_{jk} - Y_j) \times Y_j \times \frac{2(net_j)}{\sigma_j^2} \tag{22}$$

Compute parameter changes, and adjust weights using the gradient descent algorithm as follows:

$$\sigma_j(p+1) = \sigma_i(p) + \eta \times \Delta\sigma_j \tag{23}$$

$$m_j(p+1) = m_i(p) \pm \eta \times \Delta m_j \tag{24}$$

$$\begin{cases} +\eta \times \Delta m_j, & \textit{function approximation for positive slope} \\ -\eta \times \Delta m_j, & \textit{function approximation for negative slope} \end{cases} \tag{25}$$

where T_{jk} is the target output for an input training vector X_k; η is learning rate, $0 < \eta \leq 1$; and p refers to the iteration number. The initial parameter σ_j is set to 1, whereas the initial parameter m_j represents the mean values of L_1, L, and μ.

Step 4. Compute the mean squared error (MSE) term using the following equation:

$$MSE = \frac{1}{K} \sum_{k=1}^{K} (T_{jk} - Y_j)^2 \leq \varepsilon \tag{26}$$

When MSE is less than a pre-specified tolerance error ε, learning stage is terminated at this sub-learning stage.

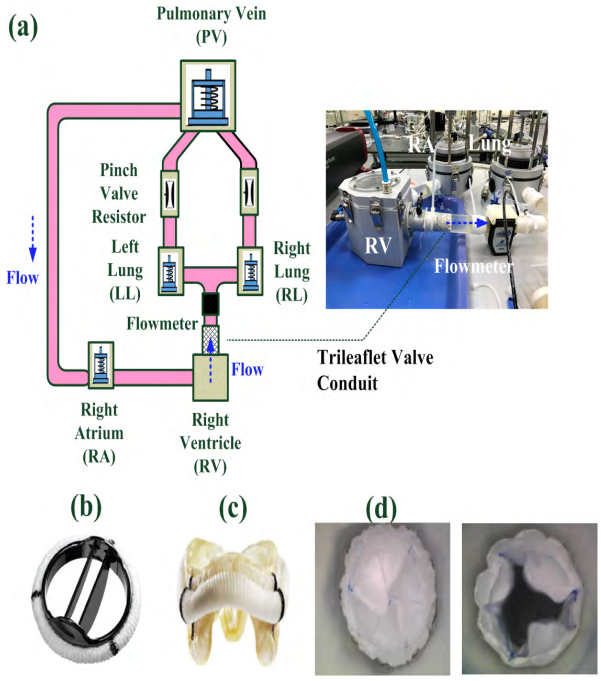

FIGURE 4. Experimental system setup and valve stents. (a) The schematic diagram of biophysical pulmonary circulation loop system, (b) Mechanical heart valve (ST. JUDE Medical), (c) Epic valve (ST. JUDE Medical), (d) Handmade trileaflet valve.

Step 5. Freeze the optimal parameters σ_j and m_j, and then connect w_{ij} from the input nodes to the candidate node. The candidate node then becomes a hidden node $Z_j = Y_j$ as follows:

$$Z = [Z_1 \times L_{1\max}, Z_2 \times L_{\max}, Z_3 \times \mu_{\max}] \tag{27}$$

Step 6. Generate a new candidate unit ($j = 2, 3, \ldots$) and repeat Step 2 until all hidden units are trained. Finally, the trained *CCN*-based machine learning estimator is used to estimate optimal leaflet parameters for the handmade trileaflet valve design.

C. EXPERIMENTAL SYSTEM SETUP

As presented in Figure 4, an experimental biophysical system is established to simulate a pulmonary circulation loop system consisting of an artificial right ventricle, a primary pulmonary artery with the right and left pulmonary branches, pinch valve resistors, a pulmonary vein, and an artificial right atrium. The artificial right ventricle can produce blood pressure waves propagating along the pulmonary arteries to the right and left lungs. Blood pressure and flow are driven by a digitally controlled hydraulic piston pump (ViViTro Labs Inc., Super Pump System, Victor, BC) to produce pulsatile waves with HRs of 60 and 80 beats/min. The artificial pulmonary artery is made of 2.0 mm-thick silicone rubbers with a T-shaped geometry, exhibits 0.2 mL/mmHg volume compliance, and connects to the right and left lung compliance chambers. The inner diameter of the primary pulmonary artery measures 25.0 mm, and the artery allows

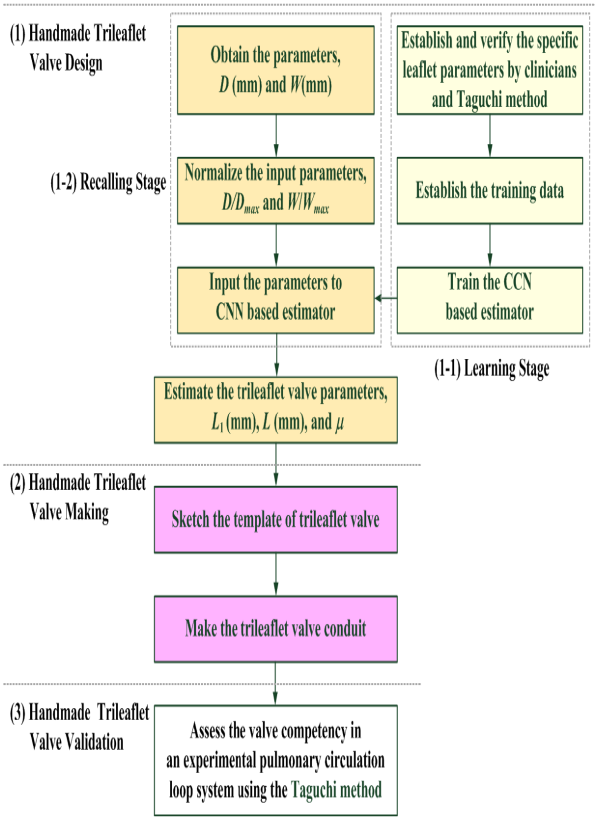

FIGURE 5. The flowchart of the design, make, and validation of the handmade trileaflet valve.

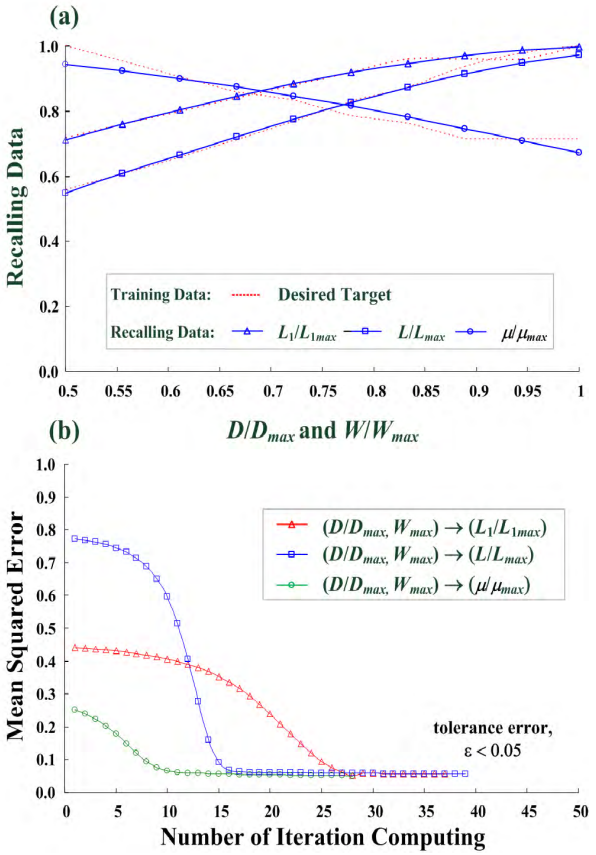

FIGURE 6. The *CCN* based estimator training. (a) Input-output paired training data for *CCN* based estimator, (b) The mean squared errors versus the number of iteration computing at each learning stage.

mimicking of blood flows of 40, 50, and 60 mL through the artificial pulmonary valve. Two sets of compliance chambers and pinch valve resistors are designed and attached to the distal ends of the right and left pulmonary arteries to mimic resistance and compliance characteristics of the distal vasculature. The blood-mimicking fluid is made from water and glycerin (water:glycerin = 1.688: 1.000; kinematic viscosity: 2.8–3.8 m^2/s; density: 1.05–1.06 kg/m^3) at 37 ± 2 °C. A handmade trileaflet valve is also constructed using ePTFE for pulmonary valve reconstruction, as illustrated in Figure 4(d).

The metering system consists of a transonic clamp-on flow sensor (ME16PXL, Transonic Systems, Ithaca, NY, USA; resolution, 10 Hz; ± 5 mL/min, bidirectional flow) and pressure transducers (81A 006G Sensormate, Chang Hau, Taiwan). These devices are employed to obtain RVP, pulmonary arterial pressure (PAP), and PAF via a data acquisition (DAQ) card (National Instruments^{TM}, PCI-6259 Austin, TX, USA) connected to a laptop PC. As shown in the experimental system in Figure 4, we compared the handmade trileaflet valved conduit with commercial valve stents, such as a mechanical heart valve and an Epic valve (Figures 4(b) and 4(c), respectively), to evaluate valve competency. Figure 5 shows a flowchart of the design, construction, and validation of the proposed handmade trileaflet valve.

III. EXPERIMENTAL RESULTS AND DISCUSSION

A. CCN BASED ESTIMATOR TRAINING PROCESS AND TESTING

According to Table 1 and Figure 6(a), architecture of the *CCN*-based estimator can be determined using input–output pairs of training data, such as the combination of (D/D_{max}, W/W_{max}) and ($L_1/L_{1\,max}$, L/L_{max}, μ/μ_{max}). With multiple regression data, hidden nodes with nonlinear radial basis functions can map the nonlinear relationship between two input variables and three output response variables for function-approximation applications. The configuration consists of two input nodes in the input layer, one hidden node in the hidden layer, and one linear output layer at each learning stage. The estimator can perform nonlinear mapping of input and target vectors. A kernel-based transformation with radial basis function transfers input patterns into the desired output scatter data for interpolation and nonlinear curve approximations. Using three batches of input–output paired training data (Figure 6(a)), the *CCN* learning procedure can quickly fit 10 paired training data created by tuning the two parameters, σ_j and m_j, and $j = 1, 2, 3$ at each learning stage. For each learning stage, the first hidden node is added to the *CCN* network by tuning parameters of the radial basis function. Other hidden nodes are added, with

TABLE 2. Optimal parameters for *CCN*-based estimator at each learning stage.

Learning Stage	Training Data	Optimal Parameter		Training Time (s)
		σ	m	
1	10	0.9344	1.0330	0.0427
2	10	1.3189	0.1832	0.0316
3	10	0.8381	1.1455	0.0244

one node per learning stage, via the same process until the maximum number is reached. Hence, three learning stages are obtained for the trained *CCN*-based estimator. In this study, the gradient descent algorithm is employed to adjust σ_j and m_j to minimize MSE at each iteration using Equations (21)–(26). For $\varepsilon < 0.05$, each learning stage can converge on a specific valve in <40 iterations, as depicted in Figure 6(b). Each learning stage requires an average of <0.0500 s of CPU time. Table 2 summarizes the determined optimal parameters. The configuration of *CCN*-based estimator is directly related to its physical applications. Given the independent training process for each batch of training data and a pre-determined number of hidden nodes, the size of *CCN* can be effectively controlled to avoid overfitting. The number of training data can also be pre-specified to establish leaflet templates for children and adults (standard template) while reducing data requirements of the *CCN*.

Based on comparisons between the *CCN* model and multilayer models, the fully connecting neural network is also selected to propose the trained estimator. We use 2 input nodes, 10 hidden nodes with radial base functions, and 3 output nodes to construct a multiple-layer nonlinear model with a network topology of 2–10–3. With the same training data, the multilayer model must adjust whole parameters, including network parameters w_{ij}, σ_j, and m_j, where $i = 1, 2$ and $j = 1, 2, 3$. The learning stage for this model requires > 200 iterations and > 2.374 s of CPU time. The proposed *CCN* model can learn quickly and provide partial learning without requiring adjustment of all network parameters at each learning stage. The proposed learning model is also employed to deal with nonlinear mapping techniques for interpolation applications. For untrained data, 17 testing data are randomly selected to verify estimation of trileaflet valve parameters, as shown by the numerical results in Table 3. Thus, we validate the proposed *CCN* model, which provides promising numerical results for the handmade trileaflet valve design.

B. HANDMADE TRILEAFLET VALVE DESIGN AND MAKING

For a pulmonary artery with an inner diameter $D' = 23.00$ mm as measured via CT pulmonary angiography, an oversized conduit diameter of $D = 23.00 \text{ mm} \times 1.15 \approx 26.50$ mm is determined. Thereafter, W of each leaflet, which is approximately one-third of the perimeter, $W = (D \times \pi)/3 \approx 27.74$ mm, is computed. Then, the *CCN*-based estimator is employed to estimate three leaflet parameters, $L_1 = 4.58$ mm, $L = 28.42$ mm, and $\mu = 1.74$. Figure 7(a) shows a template of the handmade leaflet valve. In clinical applications, surgeons can rapidly estimate leaflet parameters for reconstruction of handmade trileaflet valved conduit.

TABLE 3. Results of trileaflet valve parameter estimation.

D (mm)	W (mm)	L_1 (mm)	L (mm)	μ
19.00	19.89	3.76	21.35	1.95
19.50	20.41	3.82	21.88	1.94
21.00	21.98	4.00	23.45	1.90
21.50	22.50	4.06	23.97	1.89
23.00	24.07	4.21	25.51	1.85
23.50	24.59	4.27	26.02	1.83
25.00	26.17	4.41	27.50	1.79
25.50	26.69	4.46	27.99	1.77
27.00	28.26	4.59	29.39	1.73
27.50	28.78	4.63	29.84	1.71
29.00	30.35	4.73	31.12	1.66
29.50	30.88	4.77	31.52	1.64
31.00	32.45	4.85	32.65	1.59
31.50	32.97	4.87	33.00	1.57
33.00	34.54	4.93	33.96	1.52
35.00	35.06	4.98	34.99	1.44
35.50	36.63	4.99	35.21	1.43

After determining D and W, the trileaflet valve template can be easily estimated for children or adults using the *CNN*-based estimator. The leaflet template can be sketched using computer-aided design software, such as MATLAB, AutoCAD, or SolidWorks. In this study, we use MATLAB plotting (MathWorks, Natick, MA, USA) to sketch the template of each leaflet valve; a sample template is shown in Figure 7(a). A thin ePTFE membrane is then trimmed into bisemilunar tricuspid-shaped leaflets according to the template obtained. Afterward, the handmade trileaflet valve is attached to a stent (wire frame) to reconstruct a pulmonary valved conduit [10], [24]. A transcatheter valve delivery system is employed to deliver and to properly position the handmade trileaflet valved conduit in the heart; this conduit can expand with a balloon to push the pulmonary valved conduit open for valve implantation, as shown in Figure 7(b).

C. HANDMADE TRILEAFLET VALVE VALIDATION USING TAGUCHI METHOD

An experimental biophysical model mimicking the human pulmonary circulation system is set up in a laboratory (Heart Science and Medical Device Research Center at the National Cheng Kung University Hospital, National Cheng Kung University), as shown in Figure 4. The handmade trileaflet valved conduit, an Epic valve, and a mechanical heart valve are used to mimic pulmonary valve replacement in the experimental pulmonary circulation loop system. An endoscope inspection camera is used to capture motions of the handmade valve at a rate of 30 frames per second and evaluate the prosthetic leaflet behavior, as indicated in Figures 7(c)–7(e). In contrast to commercial valve stents, the proposed handmade valved conduit opens widely to allow forward flow through it and closes tightly to prevent regurgitation flow during each heartbeat. The dynamic motion of the proposed valve further reveals a promising opening degree for preventing thrombus formation.

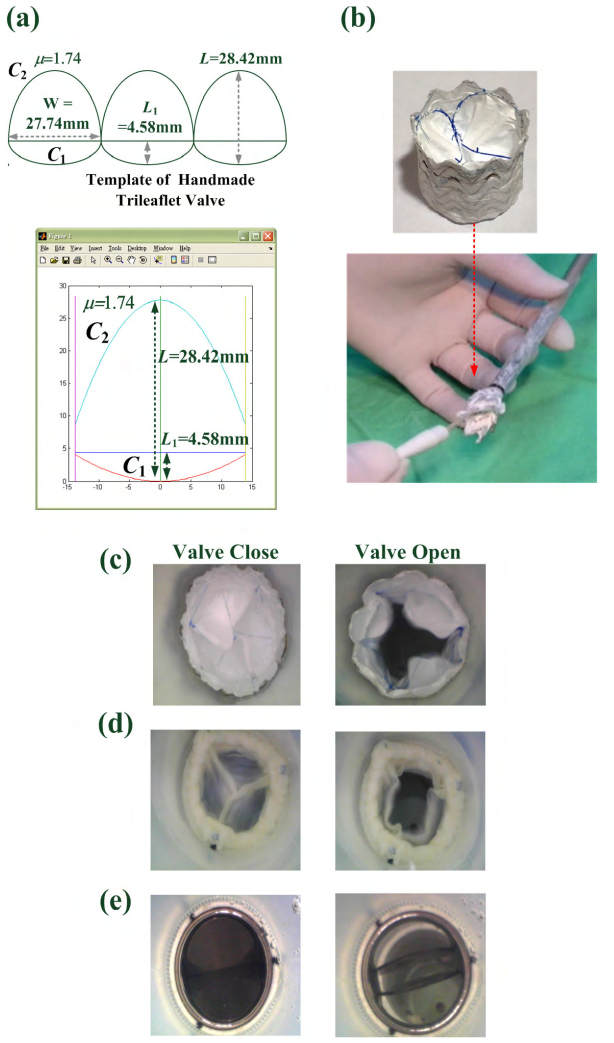

FIGURE 7. Handmade pulmonary valve stent. (a) The template of handmade trileaflet valve, (b) Hanmade trileaflet valve conduit, (c) Valve dynamic motion for e-PTFE valved conduit, (d) Valve dynamic motion for Epic valve, (e) Valve dynamic motion for mechanical heart valve.

A flow sensor and pressure transducers are also employed to obtain PAP and PAF signals via a DAQ card connected to a laptop PC over at least 1 min, as presented in the Appendix and Figure 8. Given different HRs (60 and 80 beats/min) and flow volumes (40, 50, and 60 mL), two symptoms, RVP $\geq$ 60 mmHg (hypertension) and RVP $<$ 60 mmHg (asymptomatic), are considered to examine hemodynamic conditions and valve competency. As shown in Figure 8, data on every 10 heartbeats are used to evaluate the efficacy of the valve stent. Using Equations (6)–(8) and (11)–(12), average indexes $RF\% = 15.55\% \pm 2.23\%$ ($< 20.00\%$) and $HPE\% = 84.45\% \pm 2.23\%$ ($> 80.00\%$) are respectively obtained under normal and hypertension conditions. In contrast to those of the valveless condition ($RF\% = 45.68\% \pm 1.15\%$; $HPE\% = 54.32\% \pm 1.15\%$), experimental results indicate that the handmade trileaflet valved conduit improves regurgitation flow and increases pumping efficacy of the heart, as shown in Table 4. Under asymptomatic and hypertension conditions, valve competency of the mechanical heart valve deteriorates in terms of *RF%* and *HPE%*. The mechanical heart valve demonstrates an average *RF%* of 30.78% $\pm$ 5.38% and an average *HPE%* of 69.22% $\pm$ 5.38%. By comparison, the proposed handmade valved conduit displays outcomes similar to those of the Epic valve, which is considered in this work as the gold standard, under different heartbeats, flow volumes, and hypertension conditions. The handmade trileaflet valved conduit yields mean PAP with an average systolic pressure of 24.28 mmHg and average diastolic pressure of 16.55 mmHg (normal: systolic pressure, 20–30 mmHg; diastolic pressure, 8–12 mmHg; and mean pressure, 25 mmHg); these values are comparable with those of commercial valve stents. These experimental results indicate good outcomes in terms of hemodynamic status and regurgitation improvement. Outcomes of the handmade trileaflet valved conduit also reveals significant improvement, indicating its applicability to valve replacement.

The size of the handmade trileaflet valved conduit (D = 26.50 mm, W = 27.74 mm, L_1 = 4.58 mm, L = 28.42 mm, and μ = 1.74) validates achievement of the desired target goals, i.e., $RF\% \leq 20\%$ and $HPE\% \geq 80\%$. The Taguchi method is employed to determine valve competency under different HRs, flow volumes, and hypertension conditions using S/N_{NTB}, S/N_{LTB}, and S/N_{STB}. In 12 experimental runs, the evaluations provided by this method verify the design parameters through the following steps:

- To minimize the objective function to a moderate level, i.e., $RF\% < 20\%$, S/N_{STB} is computed using Equation (9) over 12 experimental runs, as shown in Table 4;
- To maximize the objective function, i.e., $HPE\% > 80\%$,
- To obtain minimum variation in the desired, i.e., $RF\% = 20\%$ and $HPE\% = 80\%$, S/N_{NTB} is computed using Equations (10) and (14) with the mean values and standard deviations.

Table 5 shows numerical results for the proposed handmade trileaflet valved conduit and commercial valve stents, including the ratios $S/N_{RF,STB}$, $S/N_{HPE,LTB}$, $S/N_{RF,NTB}$, and $S/N_{HPE,NTB}$. For flow regurgitation improvement, the objective function is of the S/N_{STB} type. Hence, the handmade trileaflet valve (-23.93 dB) features better $S/N_{RF,STB}$ than commercial valve stents and under valveless condition. For *HPE* enhancement, the objective function is of the S/N_{LTB} type. Thus, $S/N_{HPE,LTB}$ of the handmade trileaflet valve (38.52 dB) is larger than those of commercial valve stents and under valveless condition. For minimum variation in the desired goals, i.e., $RF\% = 20\%$ and $HPE\% = 80\%$, $S/N_{RF,NTB}$ and $S/N_{HPE,NTB}$ of the proposed design (16.12 and 30.82 dB, respectively) are similar to the outcomes for the Epic valve stent. These results indicate that the Taguchi method can be used to evaluate the handmade trileaflet parameter design and validate improvements in valve replacement, especially when compared with commercial valve stents and under valveless conditions. The handmade trileaflet valve parameters can be easily designed for pulmonary valved conduit reconstruction using the

TABLE 4. Experimental results for valve competency tests with heart rates, 60 and 80 beat/min, and flow volumes, 40, 50, and 60 mL.

No.	Hypertension	Heart Rate (beat/min)	Volume (mL)	Handmade Trileaflet Valve	Epic Valve	Mechanical Heart Valve	Valveless
				RF%	*RF%*	*RF%*	*RF%*
1	×	60	40	12.22	16.12	19.50	45.24
2	×		50	11.58	13.59	20.92	44.19
3	×		60	11.97	14.35	27.92	43.28
4	×	80	40	16.09	18.83	34.73	47.55
5	×		50	16.51	19.29	33.88	46.26
6	×		60	15.01	17.25	31.24	47.04
7	○	60	40	16.36	11.91	35.62	46.33
8	○		50	16.20	17.40	33.33	45.76
9	○		60	15.75	16.57	30.43	45.41
10	○	80	40	18.69	20.90	34.61	45.86
11	○		50	18.01	19.27	33.88	45.61
12	○		60	18.24	17.99	33.31	45.62
Mean				15.55	16.96	30.78	45.68
Standard Deviation				2.23	2.62	5.38	1.15
No.	Hypertension	Heart Rate (beat/min)	Volume (mL)	Handmade Trileaflet Valve	Epic Valve	Mechanical Heart Valve	Valveless
				HPE%	*HPE%*	*HPE%*	*HPE%*
1	×	60	40	87.78	83.88	80.50	54.76
2	×		50	88.42	86.41	79.08	55.81
3	×		60	88.03	85.65	72.08	56.72
4	×	80	40	83.91	81.17	65.27	52.45
5	×		50	83.49	80.71	66.12	53.74
6	×		60	84.99	82.76	68.77	52.96
7	○	60	40	83.64	88.09	64.38	53.67
8	○		50	83.80	82.60	66.67	54.24
9	○		60	84.25	83.43	69.57	54.59
10	○	80	40	81.32	79.10	65.39	54.14
11	○		50	81.99	80.73	66.12	54.39
12	○		60	81.76	82.00	66.69	54.38
Mean				84.45	83.04	69.22	54.32
Standard Deviation				2.23	2.62	5.38	1.15

TABLE 5. Numerical results of three S/N ratios for the proposed handmade trileaflet valve conduit and commercial valve stents.

S/N \ Valve Type	Handmade Trileaflet Valve	Epic Valve	Mechanical Heart Valve	Valveless
$S/N_{RF,STB}$ (dB)	-23.93	-24.68	-29.89	-33.19
$S/N_{RF,NTB}$ (dB)	16.12	16.22	15.15	31.98
$S/N_{HPE,LTB}$ (dB)	38.52	38.37	36.74	34.69
$S/N_{HPE,NTB}$ (dB)	30.82	30.02	22.19	33.49

proposed *CCN*-based estimator. Behavior of the proposed valve is validated in the biophysical pulmonary circulation loop system and evaluated by the Taguchi method via S/N ratios. Competence of the handmade trileaflet valve can be easily implemented over a large range of diameters (e.g., 18.00–36.00 mm) for clinical use in both children and adults.

IV. CONCLUSION

In this study, a handmade trileaflet valve for pulmonary valved conduit reconstruction is designed and validated using the Taguchi method and a *CCN*-based estimator. In clinical applications, homografts, bovine jugular vein conduits, porcine valves, Epic valves, and mechanical heart valves may present possible strategies for pulmonary valve replacement. However, these devices present issues on availability, durability, and size limitation, thereby restricting their wide use in children and adults. In the present work, a *CCN*-based estimator is designed to estimate optimal trileaflet valve parameters for pulmonary valved conduit reconstruction. The *CCN* features the following advantages: (1) A minimum-sized network can be constructed for a given application using simple learning algorithms; (2) the estimator features a fast learning stage to train fed input–output paired training data; (3) it is capable of partial learning and changes network parameters with new training data; and (4) it requires a minimal number of connections, which imply faster computation times. Given D and W, the estimator determines optimal parameters, which are then used to rapidly sketch the trileaflet template by application software, as provided in the Appendix (Figure 9).

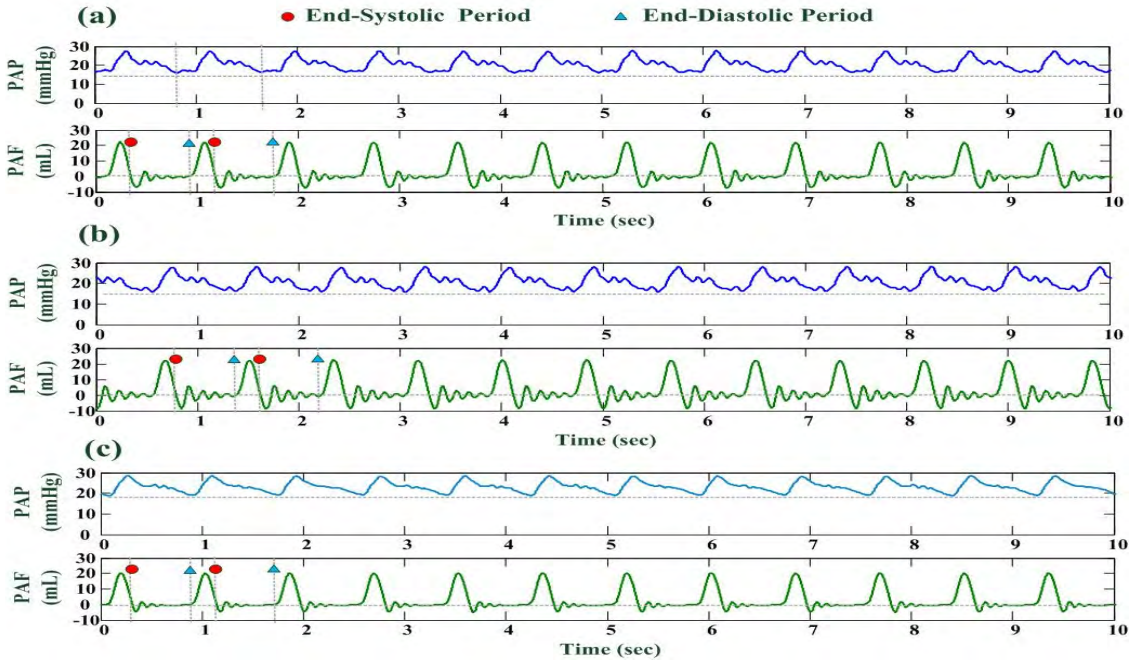

FIGURE 8. Experimental raw data with 60 beat/min, and flow volumes, 50 mL. (a) The raw data of PAP and PAF signals for handmade trileaflett valve, (b) The raw data of PAP and PAF signals for mechanical heart valve, (c) The raw data of PAP and PAF signals for Epic valve.

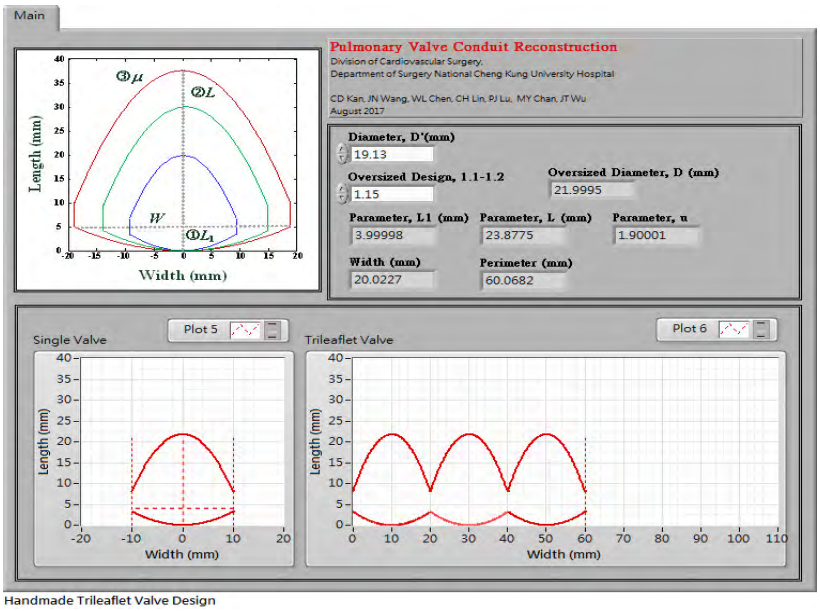

FIGURE 9. The graphic user interface (GUI) for Handmade Trileaflet Valve Design.

Thereafter, an ePTFE membrane is trimmed into bisemilunar tricuspid-shaped leaflets according to the designed template. The proposed trileaflet valved conduit exhibits good biocompatibility and low antigenicity, and valve functions are validated using an experimental pulmonary circulation loop system. In contrast to commercial valve stents, the handmade trileaflet valved conduit exhibits good performance, as evidenced by the obtainedS/N_{STB}, S/N_{LTB}, and S/N_{NTB} ratios. The proposed handmade trileaflet valved conduit can be used in clinical applications. Further in vivo animal experiments (e.g., pig models) are necessary to validate mid- and long-term effectiveness of the handmade conduit and its ability to prevent repeated heart surgery and postoperative degeneration.

APPENDIX

See Figs. 8 and 9.

REFERENCES

[1] N. Holoshitz and Z. M. Hijazi, "Transcatheter pulmonary valve replacement: Valves, techniques of implantation and outcomes," *Intervent. Cardiol.*, vol. 5, no. 4, pp. 465–477, 2013.
[2] W. A. Zoghbi *et al.*, "Recommendations for evaluation of the severity of native valvular regurgitation with two-dimensional and Doppler echocardiography," *J. Amer. Soc. Echocardiogr.*, vol. 16, no. 7, pp. 777–802, 2003.
[3] Y. Ko, K. Morita, T. Abe, M. Nakao, and K. Hashimoto, "Variability of pulmonary regurgitation in proportion to pulmonary vascular resistance in a porcine model of total resection of the pulmonary valve: Implications for early- and long-term postoperative management of right ventricular outflow tract reconstruction with resulting pulmonary valve incompetence," *World J. Pediatric Congenital Heart Surg.*, vol. 6, no. 4, pp. 502–510, 2015.
[4] M. Nakagawa *et al.*, "Characteristics of new-onset ventricular arrhythmias in pregnancy," *J. Electrocardiol.*, vol. 37, no. 1, pp. 47–53, 2004.
[5] P. Nathani, S. Shetty, and Y. Lokhandwala, "Ventricular tachycardia in structurally normal hearts: Recognition and management," *J. Assoc Phys. India, Suppl.*, vol. 55, pp. 33–38, Apr. 2007.
[6] S. G. Myerson *et al.*, "Aortic regurgitation quantification using cardiovascular magnetic resonance: Association with clinical outcome," *Circulation*, vol. 126, pp. 1452–1460, Sep. 2012.
[7] L. Søndergaard *et al.*, "Quantification of aortic regurgitation by magnetic resonance velocity mapping," *Amer. Heart J.*, vol. 125, no. 4, pp. 1081–1090, 1993.
[8] N. Honda *et al.*, "Aortic regurgitation: Quantitation with MR imaging velocity mapping," *Radiology*, vol. 186, no. 1, pp. 189–194, 1993.
[9] M. Ando and Y. Takahashi, "Ten-year experience with handmade trileaflet polytetrafluoroethylene valved conduit used for pulmonary reconstruction," *J. Thoracic Cardiovascular Surg.*, vol. 137, no. 1, pp. 124–131, 2009.
[10] T.-W. Lin, J.-N. Wang, C.-D. Kan, and Y.-J. Yang, "Handmade trileaflet valved stent graft for pulmonary valve implantation," *J. Thoracic Cardiovascular Surg.*, vol. 148, no. 4, pp. 1753–1755, 2014.
[11] M.-T. Lin, J.-K. Wang, P.-Y. Wu, C.-W. Lu, T.-I. Chang, and Y.-S. Chen, "Successful transcatheter handmade-valved graft stent for branch pulmonary regurgitation: Novel approach in a special event," *Soc. Thoracic Surgeons*, vol. 12, no. 6, p. e541-543, 2016.
[12] P. Loyalka *et al.*, "Transcatheter pulmonary valve replacement in a carcinoid heart," *Texas Heart Inst. J.*, vol. 43, no. 4, pp. 341–344, 2016.
[13] E. Yamashita *et al.*, "Smaller-sized expanded polytetrafluoroethylene conduits with a fan-shaped valve and bulging sinuses for right ventricular outflow tract reconstruction.," *Ann Thoracic Surg*, vol. 102, no. 4, pp. 1336–1344, 2016.
[14] S. M. Emani *et al.*, "Concept of an expandable cardiac valve for surgical implantation in infants and children," *J. Thoracic Cardiovascular Surg.*, vol. 152, no. 6, pp. 1514–1523, 2016.
[15] C.-H. Chiang, M.-L. Yeh, W.-L. Chen, and C.-D. Kan, "Apparatus for comparison of pullout forces for various thoracic stent grafts at varying neck angulations and oversizes," *Ann. Vascular Surg.*, vol. 31, pp. 196–204, Feb. 2016.
[16] J. Ng *et al.*, "Over-expansion capacity and stent design model: An update with contemporary DES platforms," *Int. J. Cardiol.*, vol. 221, pp. 171–179, Oct. 2016.
[17] M. D. Sulistiyo, R. N. Dayawati, and P. A. M. Pahirawan, "Iridology-based dyspepsia early detection using linear discriminant analysis and cascade correlation neural network," in *Proc. 2nd Int. Conf. Inf. Commun. Technol.*, May 2014, pp. 144–149.
[18] A. B. Nassif, L. F. Capretz, and D. Ho, "Software effort estimation in the early stages of the software life cycle using a cascade correlation neural network model," in *Proc. 13th ACIS Int. Conf. Softw. Eng., Artif. Intell., Netw. Parallel Distrib. Comput.*, Aug. 2012, pp. 589–594.
[19] Z. Yongman and H. Zhen, "Applications of cascade correlation neural networks for manufacturing process monitoring," in *Proc. 3rd Int. Conf. Inf. Manage., Innov. Manage. Ind. Eng.*, vol. 2. Nov. 2010, pp. 47–50.
[20] R. K. Roy, *Design of Experiments Using the Taguchi Approach: 16 Steps to Product and Process Improvement*. Hoboken, NJ, USA: Wiley, 2001.
[21] I. Ben-Gal, "On the use of data compression measures to analyze robust designs," *IEEE Trans. Rel.*, vol. 54, no. 3, pp. 381–388, Sep. 2005.
[22] I. Ben-Gal, R. Katz, and Y. Bukchin, "Robust eco-design: A new application for air quality engineering," *IIE Trans.*, vol. 40, no. 10, pp. 907–918, 2008.
[23] D. Fratila and C. Caizar, "Application of Taguchi method to selection of optimal lubrication and cutting conditions in face milling of $AlMg_3$," *J. Cleaner Prod.*, vol. 19, nos. 6–7, pp. 640–646, 2011.
[24] C.-D. Kan *et al.*, "Applicability of the handmade ePTFE trileaflet-valved conduits for pulmonary valve reconstruction: An *ex vivo* and *in vivo* study," *J. Thoracic Cardiovascular Surg.*, in press. doi: http://dx.doi.org/10.1016/j.jtcvs.2017.09.049
[25] C. Seiler, B. C. Aeschbacher, and B. Meier, "Quantitation of mitral regurgitation using the systolic/diastolic pulmonary venous flow velocity ratio," *J. Amer. College Cardiol.*, vol. 31, no. 6, pp. 1383–1390, 1998.
[26] P. Lancellotti *et al.*, "Recommendations for the assessment of valvular regurgitation, part 1: Aortic and pulmonary regurgitation (native valve disease)," *Eur. Assoc. Echocardiogr.*, vol. 11, no. 3, pp. 223–244, 2010.

CHUNG-DANN KAN received the M.D. degree from the Kaohsiung Medical College, Kaohsiung, Taiwan, in 1993, and the Ph.D. degree from National Cheng Kung University, Tainan, Taiwan, in 2010. He completed the Residency and Fellowship training in cardiovascular surgery at National Cheng Kung University Hospital, Tainan. He is currently an attending Physician with the Department of Surgery, National Cheng Kung University Hospital, and the Institute of Clinical and Cardiovascular Research Center, Medical College, Tainan. He is also an Associate Professor with National Cheng Kung University. His research interests include cardiac regeneration and aortic stent graft.

WEI-LING CHEN was born in 1970. She received the B.S. degree in mechanical engineering from National Cheng Kung University, Tainan, Taiwan, in 1994, the M.S. degree in biomedical engineering from National Cheng Kung University, Tainan, in 1996, and the Ph.D. degree from the Department of Biomedical Engineering, National Cheng Kung University, Tainan, in 2015. She has been with the Department of Engineering and Maintenance, Kaohsiung Veterans General Hospital, Kaohsiung, Taiwan, since 2013. Her research interests include biomedical signal processing, hemodynamic analysis, healthcare, numerical analysis, and medical device design.

CHIA-HUNG LIN was born in 1974. He received the B.S. degree in electrical engineering from the Tatung Institute of Technology, Taipei, Taiwan, in 1998, the M.S. degree in electrical engineering from the National Sun Yat-sen University, Kaohsiung, Taiwan, in 2000, and the Ph.D. degree in electrical engineering from National Sun Yat-sen University in 2004. He was a Professor with the Department of Electrical Engineering, Kao-Yuan University, Kaohsiung, from 2004 to 2017. He has been a Professor with the Department of Electrical Engineering, National Chin-Yi University of Technology, Taichung, Taiwan, since 2018.

His research interests include neural network computing and its applications, biomedical signal processing, healthcare, hemodynamic analysis, and pattern recognition.

JIEH-NENG WANG received the Doctor of Medicine degree from the Taipei Medical College in 1990 and the Ph.D. degree from the Graduate Institute of Clinical Medicine, Medical College, National Cheng Kung University, Tainan, Taiwan. He completed the Residency and Fellowship training in pediatric cardiology and pediatric critical care medicine at the National Cheng Kung University Hospital. He is currently an Attending Physician and an Associate Professor with the Department of Pediatrics, National Cheng Kung University Hospital.

He has authored over 70 papers in the SCI journals until now. His research interests include interventions in the congenital heart disease, postoperative care. He is a specialist in pediatric congenital heart disease, and he is an Active Board Committee Member in many societies, including the Taiwan Society of Pediatric Cardiology, Taiwan Society of Cardiology, and Taiwan Society of Cariovascular Interventions. He has received many awards, including the Excellent Physician in his hospital 2013, the Best Poster in APPCS 2014, and best papers in the Chinese Institute of Engineers 2016. He has been invited many times as a speaker, a panelist, and an operator for live demo event in the Asia-Pacific area.

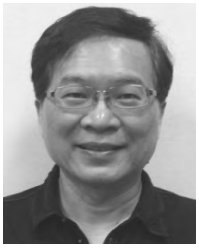

PONG-JEU LU received the B.S. and M.S. degrees in mechanical engineering from National Taiwan University, Taipei, Taiwan, in 1976 and 1978, respectively, and the Ph.D. degree in mechanical and aerospace engineering from Princeton University in 1984. He joined the Faculty of the Department of Aeronautics and Astronautics, National Cheng Kung University, in 1984, and he served as an Associated Professor, a Professor, and the Department Chairman therein. In 2000, he founded the Heart Science and Medical Devices Research Center collaborating with cardiac surgeons and cardiologists on various subjects related to a novel invention of early interventional left ventricular assist device (LVAD) termed Para-aortic Blood Pump. His research interests include aerodynamics, hemodynamics, computational fluid dynamics, LVAD design, system dynamic modeling, artificial neural networks and automated condition monitoring and fault diagnostics of active implants.

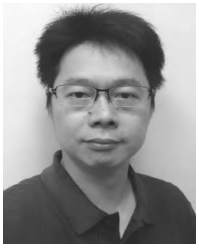

MING-YAO CHAN received the B.S. degree in aeronautical engineering form Tamkang University, New Taipei, Taiwan, and the M.S. and Ph.D. in aeronautical and astronautical engineering from the National Cheng Kung University, Tainan, Taiwan. He joined the Heart Science and Medical Devices Research Center in 2000 and participated in various projects related to design and testing a novel left ventricular assisted device and bone cement delivery system. He has been the Technology Manager of 3R Life Sciences Taiwan Ltd., Kaohsiung, Taiwan, since 2013. His research interests include hemodynamics, LVAD design, system dynamic modeling and in-vitro mock loop design and testing.

JUI-TE WU received the bachelor's degree in veterinary medicine from National Chung-Hsing University, Taichung, Taiwan, in 1998, and the Ph.D. degree in veterinary medicine from National Chung-Hsing University, Taichung, in 2006. He is currently an Assistant Professor with the Department of Veterinary Medicine, National Chiayi University. He is an attending Veterinarian of the College of Agriculuture Veterinary Teaching Hospital, National Chiayi University. His research interests include small animal surgery, dermatology, veterinary anesthesia, and veterinary reproduction and obstetrics.